Exploration of Additional Mechanical Phenomena of Laser-Tissue Interaction Contributes to the Damage and Elimination of the Small Blood Vessels

AL- Timimi Zahra'a

Abstract—This study was designed to carry out a comprehensive experimental analysis of the mechanical effects of the irradiated tissue models with nanosecond laser pulses at three different repetition frequencies are delivered using a fluence value close to the threshold fluence and, to find threshold fluence for bubble formation in a scattering tissue model.Two tissue models of agar phantoms incorporating light scattering. The first was made of a single layer, while the second, it was composed of two layers, thick layer and the scattering one, is constituted by a mixture of liquid agar gel and Intralipid. Nd:YAG laser 532 nm, pulse duration of 5 nanoseconds and a 90 femtosecond laser was used for irradiation .The result showed that permanent or transient bubbles made reckoning on the laser fluence , variety of pulses and repetition rate. Scattering added to the tissue model increased the threshold fluence for plasma formation. The permanent and transient bubble can be produced by single nanosecond laser pulses while femtosecond laser pulses were always produced transient and half the initial size than those produced with nanosecond laser pulses.

Index Terms— Nd: YAG laser, Blood Vessel, Phenomena, Bubble formation, Plasma, Threshold.

1 INTRODUCTION

Since its invention, the laser has been widely used for many applications in the field of medicine; both continuous wave (CW) and pulsed lasers are suitable for medical applications. The physical mechanisms involved in a laser-matter interaction depend, aside from wavelength, on the pulse intensity, which itself depends on the laser pulse duration; the shorter the pulse the higher the peak intensity [1, 2].

Long laser pulses (µs to ms) couple its energy to the material mainly through the wavelength dependent linear absorption, according to an extinction coefficient (µt); most of the energy deposited to the material produces heat, and therefore, the interaction is dominated by heat diffusion [3]. When the laser pulse is very intense, a fast optical and avalanche ionization process dominates the interaction and an expanding plasma is produced with a very small amount of heat transferred to the targeted material [4]. Ultra-short laser-matter interactions are, to a certain degree, wavelength-independent. While for certain transparent materials like glass there exist two distinctive "and definite trends" for the damage threshold fluence of the material for laser pulse durations above and below 10 ps, the boundary between long and ultra-short pulses is not very well established in the context for all materials, particularly biological ones [5]. Long laser pulses at convenient wavelengths have been incorporated to laser surgeries where the aim is to produce thermal (by laser heating) treatment of specific chromophores and/or tissue ablation [6].

AL- Timimi Zahra'a - Department of Laser Physics, College of Science for Women, Babylon University . E-mail:zahraja2007@yahoo.com

However, there are specific cases where the treatment is not very successful as an example, Port Wine Stain (PWS). Birthmarks are an abnormal layer of blood vessels 10 to 100µm in diameter localized 100 to 500 µm below the skin surface, that have been treated using long (1 to 2µs) laser pulses in combination with Cryogen Spray Cooling (CSC) [7-9]. This treatment has proven success with large blood vessels (~100µm), because they have a long thermal relaxation time (5µs) that allows thermal confinement in the blood vessel, hence achieving the coagulation temperature [10].

In contrast, smaller blood vessels (10µm) have shorter thermal relaxation time (50µs), which does not allow sufficient thermal confinement, hence the laser heat produced during the pulse quickly diffuses away to the surrounding tissue before the coagulation temperature is achieved and the blood vessel remains undamaged[11]. A feasible solution for this problem is the use of shorter (nano, Pico to femtosecond) laser pulses that delivers its energy faster than the thermal relaxation time of these small vessels [12]. My work in this area intended to evaluate if this approach would be feasible, but also to explore if additional mechanical phenomena could be triggered by the laser-tissue interaction, such as cavitation and shock waves, which might also contribute to the damage and the elimination of the very small blood vessels, which are difficult to remove by slow laser heating.

When a bubble is formed in an elastic medium, such as agar gels, the bubble expands and collapses several times before disappearing. However, when the plasma is very intense, the pressure inside the bubble may be so high that it plastically deforms the material producing a permanent bubble, in other words, a bubble that does not expand a collapse [10, 13].

The threshold fluence for plasma formation is the fluence at which there is 50% probability that plasma is formed. This

threshold depends on the laser pulse peak. When a laser beam is focused on the bulk of a material, it loses some energy as it propagates through because of absorption and scattering, reducing the local irradiance at the focal point [14]. It is important to find out the laser parameters that lead to plasma formation that generates a cavitation bubble in a particular material.

Such bubbles can serve as a Photodisruption mechanism for the small blood vessels that remain after traditional laser surgery with longer laser pulses. In the initial stage of the work, experiments focusing a 5 ns, Nd:YAG laser beam on agar gel artificial tissue models (phantom) was carried out [15, 16]. The threshold fluence for bubble formation was found for different absorption coefficients when the laser beam was focused at a specific depth below the surface; also, the characterization of the bubble diameter as a function of affluence was carried out for several samples with different absorption coefficients, however, only permanent bubbles were studied. Addition of dyes and intra lipids in different concentrations to agar gels allows making a more realistic skin model.

In the present work the main objectives are to study the bubble dynamics, i.e., its formation and evolution when a series of pulses at three different repetition frequencies are delivered using a fluence value close to the threshold fluence and, to find the threshold fluence for bubble formation in a scattering tissue model. The last study intends to mimic a highly scattering tissue, like skin. These experiments were carried out using a 532 nm, Nd:YAG laser, pulse duration of 5 nanoseconds and a 90 femtosecond laser.

2 MATERIALS AND METHODS

2.1 ARTIFICIAL TISSUE MODELS

Agar is typically a strong gelling polysaccharide derived from red seaweeds. Agar solutions gel due to the presence of the agarose fraction of the crude agar at common concentrations between 0.5 and 2.0%. Agar typically needs to be heated above 90 ºC to liquify (melt) and depending on the seaweed source the setting temperature can be between 30 and 45 ºC. As agar gels are mainly conformed with water, they are an excellent material to make artificial tissue phantoms [17, 18]. They may also be combined with other substances to approximate its optical properties to more realistic tissue. In this work, two types of agar phantoms were used.

Figure 1 shows the first model, which is made of a single 500 µm thick layer of transparent Agar, it was used for the experiments where the bubble dynamics were studied for different number of pulses and repetition rates. Note that the beam was focused 100µm below the surface, a typical depth at which a blood vessel can be found.

Figure 2 shows the second model, which we used to study the bubble formation in a highly scattering medium. It is composed of two layers. The top 254µm thick layers, the scattering one, is constituted by a mixture of liquid agar gel and 4.8% intra lipid; the scattering layer was stacked on top of another layer made of transparent agar gel. In this case, the laser beam was focused on (50, 100 and 200) µm deep in the scattering layer.

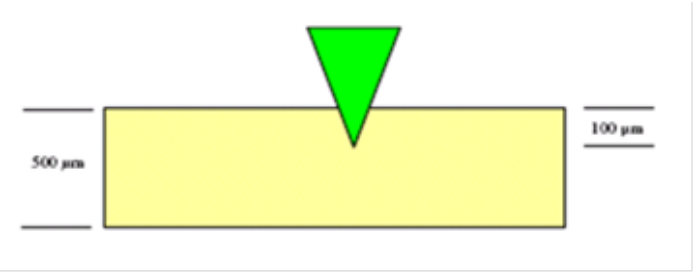

Figure 1: 500 µm Thickness transparent agar single layers

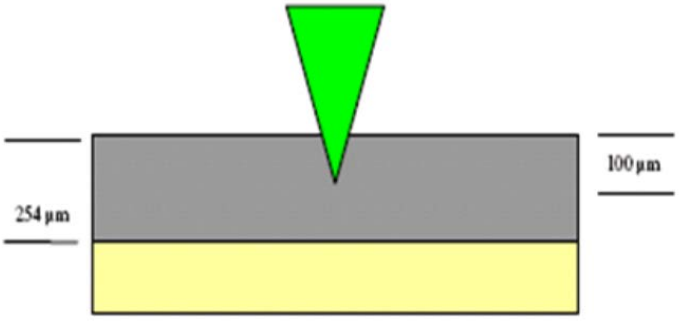

Figure 2: Highly scattering agar layer stacked on top of another layer of transparent agar

2.2 EXPERIMENTAL SETUP AND BUBBLE DETECTION

The experimental setup is shown in figure 3. It can be used in a configuration that includes both a 532nm, Nd: YAG, 5ns pulses as well as an 810nm, Ti: Sapphire, femtosecond as excitation beams and a 632.8nm, HeNe continuous wave laser as probe beam, which are focused on the target with a 0.5NA, 8mm focal length spherical lens that we will call the micro processing lens.

The energy per pulse delivered on target is monitored either with a properly calibrated photodiode and an oscilloscope or directly with an energy head detector. A CCD camera is used to capture the image of the focused beam on the target; this is done by using an image relay system constituted by the micro processing lens and 500mm lens shown in figure 3. Two lenses projecting an image of the beam waist onto the CCD collect the light that reflects backwards from the surface.

This image relay system provides three very useful features to our setup:

1. It requires normal incidence to work so that the sample surface is always perpendicular to the incident beam, and therefore, in the event of a transversal scan of the sample the beam waist of the focusing light stays always at a constant distance from the surface
2. It allows fine positioning of the beam waist right on the surface of the sample, and hence at a known depth within the layer, with a resolution of the order of the Rayleigh range of the focusing beam.
3. The same image relay system allows to record movies of the bubble formation and evolution inside the agar gel.

ISSN 2229-5518

The bubble formation dynamics is also recorded by use of the HeNe probe beam; the light transmitted through the sample is collected onto a photodiode connected to a data acquisition system. If the bubble is not present, the HeNe light detected by the photodiode produces a constant signal, however, when the bubble forms the initial constant signal drops to a minimum (when the bubbles reaches its maximum diameter) and it recovers back up as the bubble collapses.

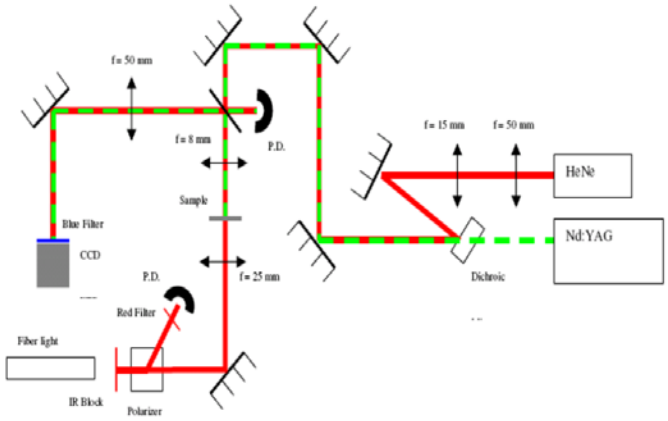

Figure 3: Experimental Setup for cavitation bubble visualization in agar gels.

2.3 Image processing

Movies of the laser-induced bubbles were taken at 10 frames per second and split into several pictures. The diameter of the bubble was measured for a selected number of pictures using standard image processing software (IMAGEJ). Figure 4 shows a typical sequence of photos of the bubble image obtained with the CCD camera.

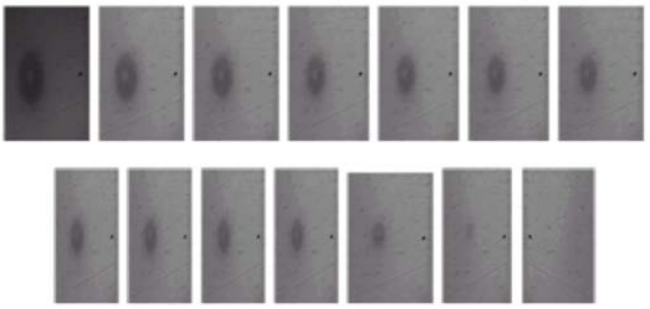

Figure 4: Typical sequence of photos that describe how the bubble diameter changes with time.The bubble was obtained by using a single 5ns (532nm) Nd:YAG laser pulse with fluence of 204.65 J/cm²

Upper row (left to right): 0 s, 0.4 s, 1.06 s, 1.73 s, 2.4 s, 3.06 s, 3.77 s.

Lower row (left to right): 4.4 s, 5.06 s, 5.73 s, 6.4 s, 9.7 s, 13.06 s, 15.5 s.

3 Results and Discussion

3.1 Bubble Dynamics

Figure 4 contains experimental results of laser irradiation of agar gel models with laser pulses of 5ns duration, at a wavelength of 532nm, on a 500µm thick transparent layer. The beam was focused 100µm deep in the agar gel layer. The data point plotted at t=0 represents the diameter of the bubble right after the last pulse.

All these experiments were carried out with fluence slightly smaller than that for the bubble formation threshold (240 J/cm²) for permanent bubbles (220.6 ± 9.6 J/cm²) such that we could generate the transient bubbles we are interested in the fluence values shown in figure 4 correspond to the average fluence value of the total number of pulses applied.

Figure 5 shows the time evolution from maximum bubble diameter when a single laser pulse is applied, each curve corresponds to different applied fluencies, which are in fact obtained from the inherent fluctuation of the laser system. Except for one case (199.16 J/cm²), it was found that the upper fluence, the larger bubble and longer period.

The case that falls off the typical trend seen in the other cases might be explained by an inhomogeneous agar gel sample. This is also suggested by the fact that for some experiments the bubble was not formed. Figure 5 shows only the cases where the bubbles were formed. Figure 4 contains the evolution of the bubble diameter for bubbles formed by a different number of pulses (1 to 10) at three different repetition rates (1, 2 and 3) Hz. Two types of distinctive bubbles were obtained.

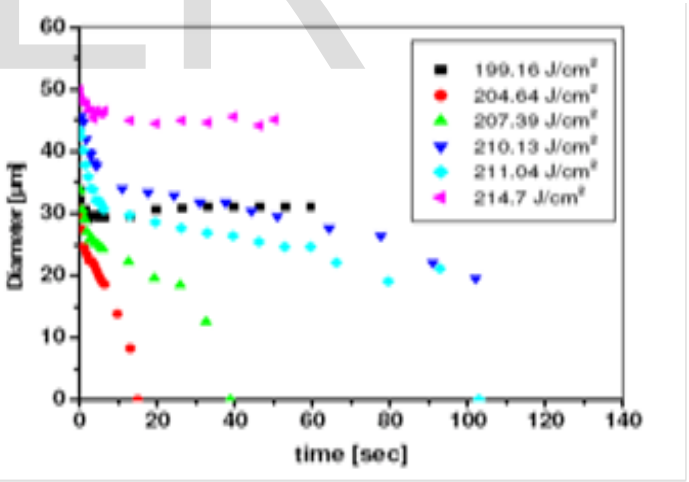

Figure 5: Bubble diameter evolution when the bubbles are created by a single 5 ns Nd:YAG laser pulse

3.2 Irradiation with Femtosecond Laser Pulses

Similar experiments were carried out irradiating transparent agar gels with bursts from Ti: Sapphire femtosecond laser pulses positioning the focal point 100µm below the gel surface, the variation of the bubble size with time is shown in figure 6.

The maximum energy used for these experiments was the maximum energy that was available with the laser system at the moment of the experiment. The fluence value shown in

figure 6 for each curve is the average fluence of two burst that produced the bubble. It should be noticed that the initial size of the bubbles is half of the maximum size obtained with nanosecond laser pulses and that all of these bubbles collapse within 20 seconds, in contrast with those produced by nanosecond laser pulses. No permanent bubbles were observed.

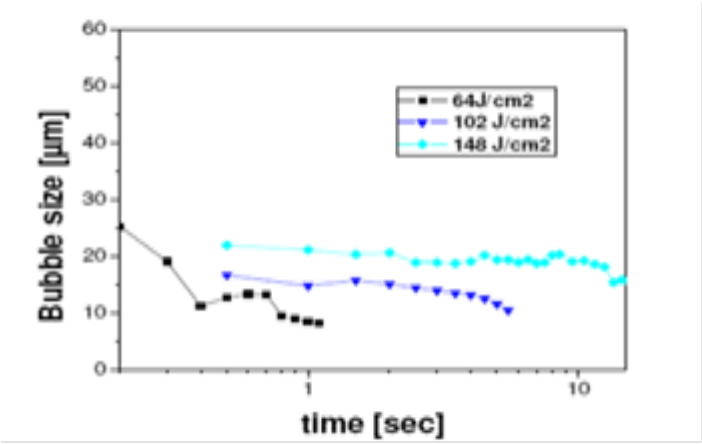

Figure 6: Bubble dynamics when bursts of femtosecond laser pulses are applied to transparent agar gels

4 Conclusion

The type of bubble (transient or permanent that can be produced by single 5 ns laser pulses is strongly dependent on the pulse fluence as shown in a previous work [18]. However, for fluences under the threshold for permanent bubble formation, the type of bubble that can be formed depends on the number of pulses and the frequency at which these are delivered [16, 19]. The fluence needed to form a bubble in highly scattering agar gel is ~50% more as that needed in clear agar gel at 50 and 100 µm deep. However, at 200µm, at least 3 times higher fluency is required. Bubbles produced with femtosecond laser pulses with the fluences available in the laboratory were always transient and half the initial size than those produced with nanosecond laser pulses.

Acknowledgments

I am extremely indebted to the School Of Physics, University Sciences Malaysia (USM), for their steerage and constant supervision additionally as for providing necessary information relating to the project & conjointly for their support in finishing the project.

References

[1] Barun, V.V. and A.P. Ivanov, *Influence of optical and thermophysical characteristics of biological tissue on its thermal conditions under laser irradiation.* Journal of Engineering Physics and Thermophysics, 2005. **78** (3): p. 422-429.

[2] Choi, B. and A.J. Welch, *Analysis of thermal relaxation during laser irradiation of tissue.* Lasers in surgery and medicine, 2001. **29** (4): p. 351-359.

[3] Lapotko, D.O., *Laserâ€ induced bubbles in living cells.* Lasers in surgery and medicine, 2006. **38** (3): p. 240-248.

[4] Niemz, M.H., *Laser-tissue interactions: fundamentals and applications*. 2007: Springer.

[5] Rubin, I.K., et al., *Optimal wavelengths for veinâ€ selective photothermolysis.* Lasers in surgery and medicine. **44** (2): p. 152-157.

[6] Stelzle, F., et al., *The impact of laser ablation on optical soft tissue differentiation of tissue specific laser surgery-an experimental ex vivo study.* J. Transl. Med. **10**.

[7] Borges da Costa, J.o., et al., *Treatment of resistant port-wine stains with a pulsed dual wavelength 595 and 1064 nm laser: a histochemical evaluation of the vessel wall destruction and selectivity.* Photomedicine and laser surgery, 2009. **27** (4): p. 599-605.

[8] Laube, S., S. Taibjee, and S.W. Lanigan, *Treatment of resistant port wine stains with the V beam® pulsed dye laser.* Lasers in surgery and medicine, 2003. **33** (5): p. 282-287.

[9] Ahçan, U., et al., *Port wine stain treatment with a dualâ€ wavelength Nd: Yag laser and cryogen spray cooling: A pilot study.* Lasers in surgery and medicine, 2004. **34** (2): p. 164-167.

[10] Tanzi, E.L. and T.S. Alster, *Comparison of a 1450â€ nm diode laser and a 1320â€ nm Nd: YAG laser in the treatment of atrophic facial scars: A prospective clinical and histologic study.* Dermatologic surgery, 2004. **30** (2): p. 152-157.

[11] Aguilar, G., et al., *Cryogen spray cooling efficiency: Improvement of port wine stain laser therapy through multipleâ€ intermittent cryogen spurts and laser pulses.* Lasers in surgery and medicine, 2002. **31** (1): p. 27-35.

[12] P©rez-Gutierrez, F., et al. *Short and Ultrashort laser pulse induced bubbles on transparent and scattering tissue models*. in *Biomedical Optics (BiOS) 2007*. 2007: International Society for Optics and Photonics.

[13] Aguilar, G., et al., *An overview of three promising mechanical, optical, and biochemical engineering approaches to improve selective photothermolysis of refractory port wine stains.* Annals of biomedical engineering. **40** (2): p. 486-506.

[14] Perez-Gutierrez, F.G., *Photomechanical, Photothermal and Photothermomechanical Mechanisms of Interaction of Nanosecond Laser Pulses With Artificial Tissue Models and Pigmented Melanoma Cells in Medical Applications.*

[15] Zhou, B., et al., *Strain rate sensitivity of skin tissue under thermomechanical loading.* Philosophical Transactions of the Royal Society A: Mathematical, Physical and Engineering Sciences. **368** (1912): p. 679-690.

[16] Rogachefsky, A.S., S. Silapunt, and D.J. Goldberg, *Nd: YAG laser (1064 nm) irradiation for lower extremity telangiectases and small reticular veins: efficacy as measured by vessel color and size.* Dermatologic surgery, 2002. **28** (3): p. 220-223.

[17] Blechinger, J.C., E.L. Madsen, and G.R. Frank, *Tissueâ€ mimicking gelatinâ€"agar gels for use in magnetic resonance imaging phantoms.* Medical physics, 1988. **15** (4): p. 629-636.

[18] Lafon, C., et al., *Gel phantom for use in high-intensity focused ultrasound dosimetry.* Ultrasound in medicine & biology, 2005. **31** (10): p. 1383-1389.

[19] Choi, B., et al. *In vivo results using photothermal tomography for imaging cutaneous blood vessels*. in *NDE for Health Monitoring and Diagnostics*. 2003: International Society for Optics and Photonics.